Atomic final state effects and a limit for time-reversal invariance in ^{191}Ir

J. L. Gimlett, H. E. Henrikson, N. K. Cheung,* and F. Boehm
Norman Bridge Laboratory of Physics 161-33, California Institute of Technology, Pasadena, California 91125
(Received 2 April 1981)

An experiment has been performed to test the time-reversal symmetry in the emission of the mixed $E2$ and $M1$ 129 keV γ transition in ^{191} Ir. The phase angle associated with the imaginary part of the ratio of multipole transition amplitudes was measured through observation of the angular distribution of the linear polarization of the γ rays from a ^{191}Os source polarized at low temperature (20 to 30 mK obtained with a dilution refrigerator). A Compton polarimeter was used to measure linear polarization. Interaction of the γ ray with the surrounding atomic electrons is expected to give rise to a phase shift ξ indistinguishable from the time-reversal phase η. In the present experiment we have observed a phase angle $(\eta + \xi) = (-4.8 \pm 0.2) \times 10^{-3}$ for the 129 keV γ ray. This value is in good agreement with the most recent calculations of the atomic final state interaction $\xi = (-4.3 \pm 0.4) \times 10^{-3}$. Assuming the validity of the calculated ξ, a limit $|\eta < 10^{-3}$ is inferred, consistent with time-reversal invariance.

[RADIOACTIVITY ^{191}Os; measured linear polarization of 129 keV from polarized nuclei, time-reversal test. Deduced relative phase of $E2$, $M1$. Relate to atomic final state effect.]

I. INTRODUCTION

The discovery of charge conjugation-parity (CP) violation, and consequently time-reversal (T) violation, in the decay of the neutral kaon[1,2] has prompted the investigation of time-reversal invariance with increasingly higher accuracy in other systems, especially in the area of nuclear physics. Among the most sensitive tests of time-reversal invariance are correlation experiments involving nuclear radiation.[3]

In a nuclear electromagnetic transition with multipoles $L\pi$ and $L'\pi'$, time-reversal noninvariance manifests itself as a relative phase shift between the transition amplitudes of the two competing multipoles. This phase, $\eta = \eta(L\pi) - \eta(L'\pi')$, is related to the mixing ratio δ by

$$\delta = \pm |\delta| e^{i\eta} \ . \tag{1}$$

A nonvanishing value of η would constitute evidence for a time-reversal violation.[4]

The imaginary component of δ (i.e., $\sin\eta$) appears in observables which change sign under a time-reversal transformation. The T-odd correlation between the vector observables $\langle \vec{J} \rangle$, $\vec{k}$, and $\vec{E}$,

$$(\langle \vec{J} \rangle \cdot \vec{k} \times \vec{E})(\langle \vec{J} \rangle \cdot \vec{k})(\langle \vec{J} \rangle \cdot \vec{E}) \ , \tag{2}$$

has been shown[5,6] to be particularly well suited for precise experimental studies of time-reversal invariance. Here $\langle \vec{J} \rangle$ is the expectation value of the spin of a nucleus in an initial (excited) state and $\vec{E}$ is the linear polarization vector of a γ ray with momentum $\vec{k}$ emitted from that state.

As the precision of such experiments improves, small quantum electrodynamic effects may become important. Hannon and Trammell[7] (and Henley and Jacobsohn[8] in reference to nuclear interactions) first pointed out that the interaction of the radiated photon with the surrounding atomic electrons can give rise to a spurious phase shift which is indistinguishable from the time-reversal phase η in a correlation experiment. These processes, often referred to as the "final state interaction," are shown schematically in Fig. 1. Diagram (a) represents the amplitude $T_{fi}(L\pi)$ for emission of a photon of multipolarity $(L\pi)$ in the deexcitation of a nucleus in in-

initial state i to final state f. The virtual interaction of the photon with a bound atomic electron is represented in lowest order by diagrams (b) and (c), for which the transition amplitude may be written[9]

$$\Delta T_{fi}(L\pi) = T_{fi}(L\pi)[\rho(L\pi) + i\xi(L\pi)] \ , \quad (3)$$

with ρ and $\zeta << 1$. The total transition amplitude is

$$T'_{fi}(L\pi) = T_{fi}(L\pi) + \Delta T_{fi}(L\pi)$$
$$\approx T_{fi}(L\pi)e^{i\xi(L\pi)} \ ,$$

modifying the mixing ratio of Eq. (1) to become

$$\delta = \pm \, |\delta| \, e^{i(\eta+\xi)} \ , \quad (4)$$

with $\xi = \xi(L\pi) - \xi(L'\pi')$. The phase shift to be observed in correlation experiments is thus $(\eta + \xi)$ rather than η.

In general, the parameters $\xi(L\pi)$ depend upon the multipolarity and energy of the nuclear transition. Goldwire and Hannon[10] have calculated these phase shifts treating the two processes of virtual internal conversion and virtual Thomson scattering of nuclear radiation off atomic electrons. Tables of the conversion and scattering components ξ_C and ξ_R have been presented for various multipole transitions at different energies and atomic numbers.

To illustrate the general results of the calculations, we show in Fig. 2 the phase shifts $-[\xi_C(E2) - \xi_C(M1)]$ and $[\xi_R(E2) - \xi_R(M1)]$ between $E2$ and $M1$ multipoles as a function of Z, for energies of 100 and 200 keV. The shift due to Thomson scattering is relatively insensitive to energy. As indicated, the phase $\xi = \xi_C + \xi_R$ is largest at low energies and for $Z \simeq 60$ and is smallest for high energy, low Z transitions.

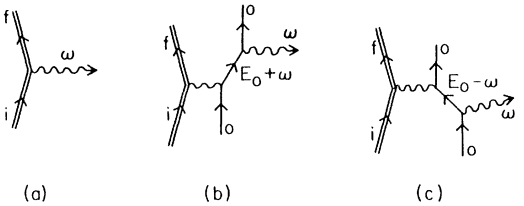

FIG. 1. Diagrammatic contributions to the photon emission amplitude for a nuclear transition. The single straight lines in (b) and (c) represent an atomic electron with initial and final state 0.

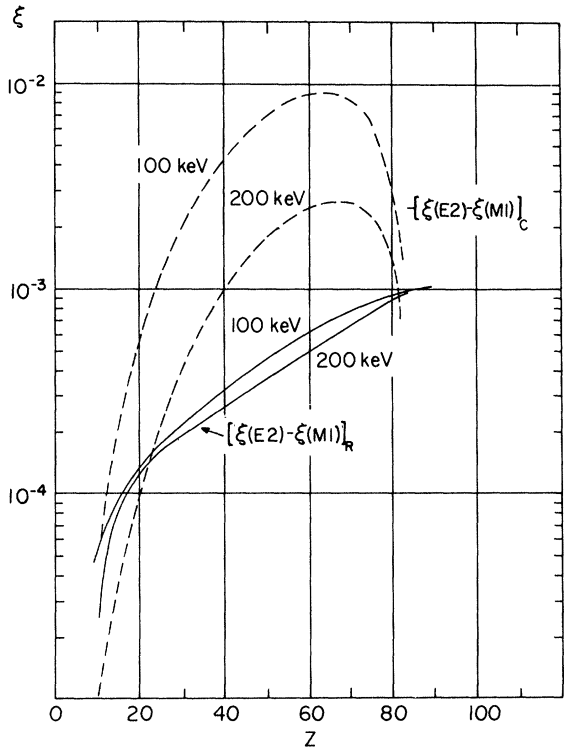

FIG. 2. Phase shifts ξ arising from atomic processes versus atomic number Z. Conversion and scattering phase shifts ξ_C and ξ_R are shown for energies of 100 and 200 keV.

As explicitly illustrated by Eq. (4), the understanding of final state effects and a precise knowledge of ξ is a prerequisite for the analysis of time-reversal studies in nuclear transitions. Aside from this practical aspect, the investigation of these quantum electrodynamical corrections is of importance in its own right.

In this paper we describe the results of an experiment based on the precise measurement of the T-odd correlation Eq. (2) in the polarization distribution of radiation emitted from nuclei polarized at low temperature. To test the calculations of Ref. 10, a case with a large expected final state interaction, the mixed $E2$-$M1$ transition of 129 keV in ^{191}Ir, has been studied. A preliminary account of the experiment, reporting the first precise measurement of a nonzero phase for the matrix-element ratio δ, has been given earlier.[11] The results of this experiment have motivated a revised calculation of final state phase shifts by Davis *et al.*[9] which incorporates a more precise Hartree-Fock treatment of the bound and continuum electron wave functions,

and includes the so-called "anomalous" scattering contribution to virtual Rayleigh scattering in the calculation of ξ_R.

II. PRINCIPLES OF THE EXPERIMENT

A. Angular distribution from oriented nuclei

The angular distribution of gamma radiation emitted from an axially symmetric oriented source may be written as a sum of three terms[6,12,13]:

$$W(\theta,\phi) = W_1(\theta) + W_2(\theta,\phi) + W_3(\theta,\phi), \quad (5)$$

where θ is the angle between the emission vector $\vec{k}$ and orientation vector $\vec{J}$, and ϕ is the angle between the polarization vector $\vec{E}$ and the $\vec{J} - \vec{k}$ plane.

The directional (intensity) distribution is given by

$$W_1(\theta) = \sum_{\lambda=\text{even}} Q_\lambda B_\lambda(I) U_\lambda A_\lambda P_\lambda(\cos\theta). \quad (6)$$

In this expression B_λ is the orientation tensor which depends on the initial nuclear spin I and the Boltzmann exponent ($\mu B/IkT$), U_λ and A_λ are deorientation and angular distribution coefficients, respectively, P_λ is the Legendre polynomial of order λ, and Q_λ is the solid angle correction. The B_λ, U_λ, and A_λ coefficients are tabulated, for example, by Krane.[14,15]

$W_2(\theta,\phi)$ and $W_3(\theta,\phi)$ are the T-even and T-odd linear polarization distribution components, respectively,

$$W_2(\theta,\phi) = \sum_{\lambda=\text{even}} Q_\lambda B_\lambda U_\lambda A_{\lambda 2} 2 \left[\frac{(\lambda-2)!}{(\lambda+2)!}\right]^{1/2} \times P_\lambda{}^2(\cos\theta)\cos 2\phi, \quad (7)$$

$$W_3(\theta,\phi) = \sum_{\lambda=\text{odd}} Q_\lambda B_\lambda U_\lambda A'_{\lambda 2}(2i) \left[\frac{(\lambda-2)!}{(\lambda+2)!}\right]^{1/2} \times P_\lambda{}^2(\cos\theta)\sin 2\phi. \quad (8)$$

The coefficients $A_{\lambda 2}$ and $A'_{\lambda 2}$ are defined by

$$A_{\lambda 2} = \frac{-E_p}{2}[-f_\lambda(LL)F_\lambda(LLI_fI_i) + 2\,|\delta|\,e^{in\pi}\cos(\eta+\xi)f_\lambda(LL')F_\lambda(LL'I_fI_i) + |\delta|^2 f_\lambda(L'L')F_\lambda(L'L'I_fI_i)]/(1+|\delta|^2), \quad (9)$$

$$A'_{\lambda 2} = \frac{-E_p}{2}[-2i\,|\delta|\,e^{in\pi}\sin(\eta+\xi)f_\lambda(LL')F_\lambda(LL'I_fI_i)]/(1+|\delta|^2) \quad (10)$$

for a linear-polarization detection system of efficiency E_p, with

$$f_\lambda(LL') = \begin{bmatrix} L & L' & \lambda \\ 1 & 1 & -2 \end{bmatrix} \Big/ \begin{bmatrix} L & L' & \lambda \\ 1 & -1 & 0 \end{bmatrix},$$

where $n = 0$ or 1 in the expression $|\delta|\,e^{in\pi}$.

The lowest-order nonzero T-violating term ($\lambda = 3$), corresponding to the vector combination of Eq. (2), becomes

$$W_3(\theta,\phi) = RQ_3B_3E_p \left[\frac{|\delta|\,e^{in\pi}}{(1+|\delta|^2)}\right] \times P_3{}^2(\cos\theta)\sin 2\phi\,\sin(\eta+\xi), \quad (11)$$

with

$$R = -(1/\sqrt{30})U_3 f_3(LL')F_3(LL'I_fI_i).$$

$W_3(\theta,\phi)$ changes under the transformation $\theta \to \pi - \theta$, $\phi \to \pi + \phi$ (equivalent to a reversal of the nuclear polarization vector $\vec{J}$), and is a maximum for $\theta_m = 54.7° \pm n\pi$, $\phi_m = 45° \pm n\pi/2$. The phase $(\eta + \xi)$ may be determined by measuring the "time-reversal" asymmetry

$$A = \frac{W(\theta_m,\phi_m) - W(\pi-\theta_m,\phi_m)}{W(\theta_m,\phi_m) + W(\pi-\theta_m,\phi_m)} = \frac{W_3}{W_1}, \quad (12)$$

with

$$W_1 = 1 + Q_4B_4U_4F_4P_4(\cos\theta_m)\,|\delta|^2/(1+|\delta|^2).$$

(Note that W_2 and the $\lambda = 2$ term of W_1 vanish at the optimum angles θ_m,ϕ_m.)

A Compton polarimeter[6] was used to measure the linear polarization of the γ radiation. The po-

larimeter efficiency E_p is defined by

$$E_p \equiv \frac{\frac{d\sigma}{d\Omega}(\rho = 90°,\Psi = 0°) - \frac{d\sigma}{d\Omega}(\rho = 90°,\Psi = 90°)}{\frac{d\sigma}{d\Omega}(\rho = 90°,\Psi = 0°) + \frac{d\sigma}{d\Omega}(\rho = 90°,\Psi = 90°)} \tag{13}$$

averaged over solid angles, where $d\sigma/d\Omega$ is the differential cross section for Compton scattering, ρ is the scattering angle, and Ψ is the angle between the initial plane of polarization and the scattering plane. Linearly polarized radiation is preferentially scattered perpendicular to its plane of polarization, and therefore E_p is negative as defined by Eq. (13).

B. Level scheme of ^{191} Ir

For a precise experimental check of the calculations,[9,10] a transition with a large expected final state phase ξ is desired. This requirement is approximately satisfied for transitions of energy $E < 200$ keV and atomic number $Z > 40$. Maximizing the sensitivity of the measured asymmetry A results in the additional criteria of a high degree of attainable polarization (i.e., $\Delta/T = \mu B/IkT$ on the order of unity), optimum multipole mixing ($\delta \approx 1$), and favorable values for the spin coefficients. In addition, the inherently poor energy resolution of the Compton polarimeter necessitates a relatively simple decay scheme. The 129 keV transition in ^{191}Ir was selected as an optimum choice for the investigation of final state effects.

The level scheme of ^{191}Ir is shown in Fig. 3. An isomeric state at 171 keV with 5-s half-life is populated in the β^- decay of ^{191}Os and cascades down to the 129 keV level. The 41.9 keV γ ray ($E3$) is

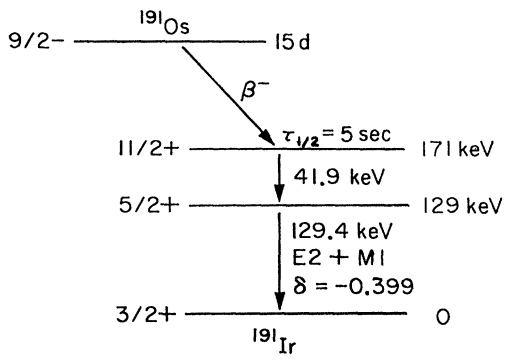

FIG. 3. Decay scheme of ^{191}Os.

internally converted and does not contribute to the spectrum. From NMR measurements the 171 keV state is known to have a magnetic moment $\mu = 5.72 \pm 0.03\ \mu_N$.[17] With an internal field for Ir in Fe of -1.481 ± 0.004 MG (Refs. 16,17) the energy splitting is $\Delta = \mu B/Ik = -56.3 \pm 0.3$ mK. Low temperatures may be obtained with a dilution refrigerator, resulting in large polarization. A mixing ratio $\mathrm{Re}\delta \simeq |\delta| e^{i\pi} = -0.399 \pm 0.004$ is reported[18] for the 129 keV transition.

III. EXPERIMENTAL METHODS

A. Source preparation

^{191}Os was produced by neutron capture in a 10 mg metallic, isotopically enriched sample of ^{190}Os sealed in an evacuated quartz capsule. The sample was encased in a 300 mg iron container and melted in an induction furnace in argon atmosphere. The resulting 1 at. % iron-osmium alloy was polished to remove surface oxide contamination, and by succesive rolling and annealing a thin foil less than 0.025 mm thick was obtained. Disks of 0.32 cm diameter were punched, polished, and finally annealed at 800 ° C in hydrogen atmosphere.

B. Cryogenic apparatus

A finished disk, with activity of 0.5 to 1.0 mCi, was indium soldered in a horizontal plane to the oxygen-free copper collar button (in one run a platinum collar button was tried to minimize magnetostrictive effects), attached to the cooling rod of a dilution refrigerator,[19] and cooled to about 25 mK. Two orthogonal pairs of superconducting Helmholtz coils thermally anchored to the 4 K shield and centered about the source provided a 2 kG external field saturating the iron foil. The ^{191}Ir nuclei are polarized via the large magnetic hyperfine interaction experienced by Ir in the Fe host. Because electronic relaxation times are short compared to the 5-s half-life,[17] full nuclear orientation is achieved in the 171 keV state.

C. Experimental setup

The physical setup of the experiment (see also Ref. 6) is shown in Fig. 4. The Compton polarimeter consists of four NaI(Tl) counters mounted at 90° from each other in a plane about an aluminum scatterer which is fixed at an angle $\theta = \theta_m = 54.7°$ from the (horizontal) $\vec{B}$ field axis. Radiation scat-

tered at 90° is detected. A 0.9 mm thick Sn absorber located before the scatterer preferentially attenuates Ir x rays with respect to the 129 keV γ ray. The four-pronged detector assembly is free to rotate through an angle $0 \leq \phi \leq 360°$ about its axis of symmetry. The pedestal supporting the polarimeter may be rotated through an arbitrary azimuthal angle $0 \leq \psi \leq 360°$ about its own axis coincident with the (vertical) axis of cooling rod and source. The four ψ positions corresponding to the axes of the orthogonal coil pairs were designated as N, S, E, and W. An intrinsic germanium (Ge) detector, used to monitor the intensity distribution $W_1(\theta)$ of the source, is supported by a carriage that rolls on a circular track concentric with the pedestal. It was generally positioned at 180° from the polarimeter.

To eliminate magnetic influences on the photomultipliers, each NaI crystal is optically coupled by means of a 30 cm lucite light pipe to its magnetically shielded phototube. The amplified outputs from the four photomultipliers provide the input to both a Northern TN1700 multichannel analyser and to four single channel analysers. In practice single-channel analyzer (SCA) output was used almost exclusively in data analysis and the pulse height spectra used to monitor detector performance and background behavior.

Alignment of source, superconducting coils, and polarimeter was maintained to within 0.02 mm, typically. Refrigerator movement with respect to the collimator was monitored by a position-sensitive indicator attached to the polarimeter, and if necessary was corrected with the three stabilizing struts which fixed the refrigerator to the rails supporting the polarimeter. Data acquisition was interrupted at 12 and 24 h intervals to fill the nitrogen and helium reserviors of the refrigerator.

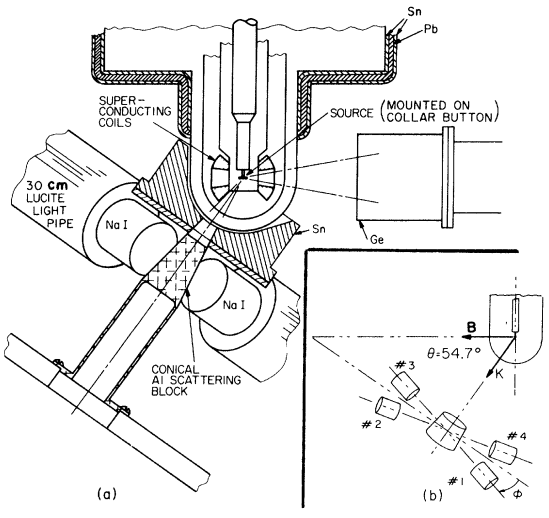

FIG. 4. Geometry of the Compton polarimeter relative to source and magnets. Only two of the four NaI detectors of the polarimeter are shown in the main diagram.

D. Determination of source temperature and nuclear orientation

To determine the source temperature, and hence the degree of nuclear orientation, the following procedures were adopted. Every 24 or 48 h the directional distribution of the 129 keV γ ray in the plane of the source was measured with the Ge detector. By measuring peak count rates in the pulse height spectra with the magnetic field applied both parallel and perpendicular to the axis of the detector a precise determination of the anisotropy ratio $W_1(\theta = 0°)/W_1(\theta = 90°)$ was obtained. The orientation coefficients

$$B_\lambda = [(2I+1)(2\lambda+1)]^{1/2} \times \frac{\sum_{m=-I}^{I} (-)^{I+m} \begin{pmatrix} I & I & \lambda \\ -m & m & 0 \end{pmatrix} e^{m\Delta/T}}{\sum_{m=-I}^{I} e^{m\Delta/T}},$$

and thus the temperature T, could in principle be calculated were it not for the partial nonalignment[20] of the Ir nuclei in Fe. An independent determination of temperature was therefore necessary. After completion of an experiment a (^{60}Co)Fe foil was indium soldered to the (^{191}Os)Fe source. The observed 129 keV anisotropy was then calibrated as a function of source temperature obtained from the known[21,22] distribution of the (^{60}Co)Fe. The partial nonalignment of ^{191}Ir was empirically treated as being the result of one or both of two possible phenomena: (1) microscopic inhomogeneities resulting in a fraction of the nuclei experiencing a small or vanishing field while the remainder sees the correct hyperfine field, and (2) an overall reduction in the hyperfine field saturation value experienced by all nuclei. A two-parameter fit of temperature to the observed 129 keV ratio $W_1'(0)/W_1'(90)$, with

$$W_1'(\theta) = 1 + \sum_{\lambda=2,4} Q_\lambda f_a B_\lambda (f_s \Delta/T) U_\lambda A_\lambda P_\lambda(\cos\theta), \quad (14)$$

yielded the free parameters f_a (the fraction of properly sited Ir nuclei experiencing the 1.481 MG field) and f_s (the degree of magnetic saturation). It was found that $f_a = 0.940 \pm 0.005$ and $f_s = 0.99 \pm 0.02$ for all but one source, which suffered from an unexplained reduction in magnetic saturation with $f_a = 0.957 \pm 0.005$ and $f_s = 0.75 \pm 0.02$.

The anisotropy measurements $W_1(0)/W_1(90)$ obtained with the Ge detector were then reanalyzed in terms of this effective distribution $W_1'(\theta)$ which replaces $B_{2,4}(\Delta/T)$ with $f_a B_{2,4}(f_s \Delta/T)$. From these even coefficients the source temperature as a function of time was determined for each experiment, and an effective third order polarization coefficient $B_3(\text{eff}) = f_a B_3(f_s \Delta/T)$ was calculated. [Other models[20] could have been chosen to describe the incomplete polarization of (Ir)Fe. As the parameters f_a and f_s assume values near unity, however, the calculation for B_3 is fairly model independent.] $W(\theta = 0°)$ was continuously monitored with the Ge detector concurrent with the time-reversal data aquisition as a check on source temperature stability.

E. Determination of polarimeter efficiency

1. Measurement from oriented ^{191}Ir

The efficiency E_p of the polarimeter for detecting linearly polarized radiation was determined from measurements of the asymmetry

$$A_p' = \frac{W'(\theta,\phi = 0°) - W'(\theta,\phi = 90°)}{W'(\theta,\phi = 0°) + W'(\theta,\phi = 90°)} = \frac{W_2}{W_1} \ , \tag{15}$$

at $\theta = 54.7°$ and 90 °. The rates $W'(\theta,\phi)$ represent the total counts in a single channel window extending from 30 to 150 keV and including the scattered ^{191} Ir line, (unresolved) Ir x rays, and background, as shown in Fig. 5(a).

The background in the polarimeter spectrum consists primarily of radiation from the source seen by the NaI counters directly through the shielding. This radiation is comprised of a small amount of the 129 keV γ ray (contributing a few percent to the total spectrum) and in the case of two later runs a sizable amount of 300 keV radiation from ^{192}Ir contaminants in the source. Because of asymmetric absorption by the superconducting coils and the anisotropic emission from oriented ^{191}Ir and ^{192}Ir, such direct radiation will produce a background asymmetry A_B in the efficiency measurement. The measured asymmetry A_p' is then a linear combination of the efficiency asymmetry A_p^* for the scattered 129 keV line (plus unresolved x rays) and the background asymmetry:

$$A_p' = (A_p^* + A_B f)/(1 + f) \ ,$$

with $f \equiv N_B/N_S$, the ratio of background (N_B) to Compton-scattered "signal" (N_S) in the spectrum. Solving for A_p^* gives

$$A_p^* = A_p'(1 + f) - A_B f \ .$$

The asymmetry A_B can be estimated from efficiency measurements obtained with the aluminum scatterer removed.

The x rays, comprising some 6% of the scattered signal, dilute the measured effect, so that

$$A_p^* = A_p(129 \text{ keV})/(1 + g) \ , \tag{16}$$

with $g \equiv N_x/N_\gamma$, the ratio of scattered x rays to scattered 129 keV gamma rays. The factor g is

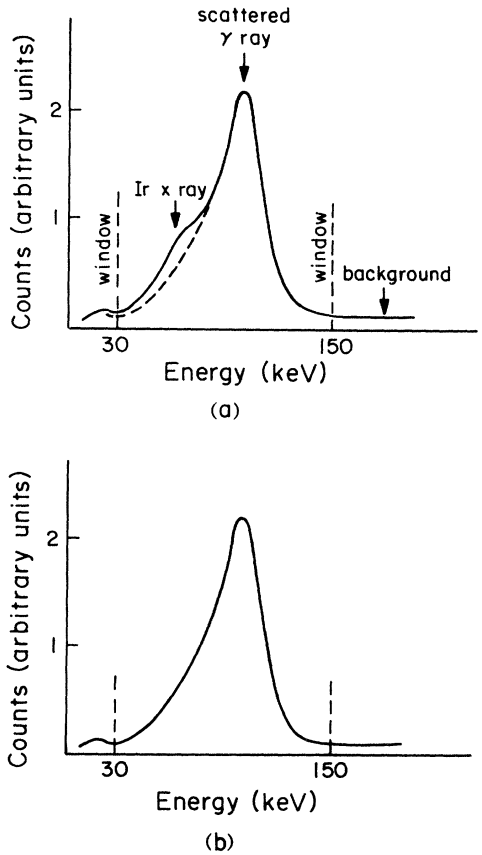

FIG. 5. NaI spectra of the Compton-scattered 129 and 122 keV lines of (a) ^{191} Ir and (b) ^{57} Fe. SCA windows are indicated.

common to both the polarization measurement (at $\theta = 54.7°$) and the measured time-reversal asymmetry A^*, and does not influence the result for $\sin(\eta + \xi)$ since

$$\sin(\eta + \xi) \propto A/E_p = A^*(1+g)/E_p^*(1+g) = A^*/E_p^* . \quad (17)$$

We may therefore speak of an effective polarization efficiency E_p and drop the asterisks.

From Eqs. (7), (9), and (15), we obtain for the polarization asymmetries

$$A_p(\theta = 54.7°) = E_p \frac{0.0606 Q_2 f_a B_2 - 0.0195 Q_4 f_a B_4}{1 - 0.0136 Q_4 f_a B_4} , \quad (18)$$

$$A_p(\theta = 90°) = E_p \frac{0.0909 Q_2 f_a B_2 - 0.0219 Q_4 f_a B_4}{1 - 0.365 Q_2 f_a B_2 + 0.0132 Q_4 f_a B_4} . \quad (19)$$

The solid angle corrections Q_λ for the polarimeter are $Q_2 = 0.982$, $Q_3 = 0.963$, and $Q_4 = 0.940$.[6] Effective orientation coefficients for B_λ have been incorporated.

To measure $A_p(\theta = 54.7°)$ the polarimeter was physically rotated to four positions corresponding to $\phi = 0°$, 90°, 180°, and 270°, and A_p' was taken to be

$$A_p'(\theta = 54.7°) = \frac{\sum_{NaI=1}^{4} W_i'(\phi = 0) + W_i'(180) - W_i'(90) - W_i'(270)}{\sum_{NaI=1}^{4} W_i'(0) + W_i'(180) + W_i'(90) + W_i'(270)} . \quad (20)$$

Averaging over the four counters and four positions in this manner served to cancel out small geometric effects. Efficiency measurements were performed at $T = 24.2$ mK, for which $f_a B_2 = 1.54$, $f_a B_4 = 0.99$, and $A_p(54.7°) = (0.0744 \pm 0.0037) E_p$. (The proportionality constant relating A_p to E_p is quite sensitive to a deviation in mixing ratio δ; hence the 5% uncertainty.) For a raw asymmetry $A_p' = -0.0333 \pm 0.0004$, a background-corrected value $A_p = -0.0315 \pm 0.0025$ was deduced, yielding $E_p = -0.42 \pm 0.04$ for the polarization efficiency.

For efficiency measurements at $\theta = 90°$, the polarimeter may remain stationary while the polarizing field is rotated 90°. (One must, however, correct for the difference in the proportion of x rays in the 90° spectrum relative to the x-ray fraction at $\theta = 54.7°$.) This procedure yielded $E_p = -0.44 \pm 0.04$.

2. *Measurement from oriented ^{57}Fe*

The accuracy of the polarization efficiency measurements with ^{191}Ir suffers from the small proportionality coefficient relating the measured asymmetry to E_p, the sensitivity of this coefficient to δ, and the sizable background corrections required. To reduce the uncertainty of E_p, the efficiency of the polarimeter was also measured using the 122 and 136 keV transitions in ^{57}Fe from the decay of oriented ^{57}Co. This source has the advantage of having a large measurable asymmetry A_p, no unresolved x rays, and no high energy radiation from ^{192}Ir contaminants. Corrections for asymmetric background are negligible.

Assuming a relative intensity ratio[6] of 89:11 between the 122 and 136 keV lines, the efficiency asymmetries for ^{57}Fe are[6]

$$A_p(\theta = 54.7°) = \frac{E_p(0.287 B_2 + 0.018 B_4)}{(1 + 0.012 B_4)} , \quad (21)$$

$$A_p(\theta = 90°) = \frac{E_p(0.430 B_2 - 0.020 B_4)}{(1 - 0.029 B_2 - 0.012 B_4)} . \quad (22)$$

Measurements of $A_p(54.7°) = -0.0986 \pm 0.0025$ and $A_p(90°) = -0.149 \pm 0.004$ at $T = 18$ mK yielded $E_p = -0.471 \pm 0.012$ and $E_p = -0.466 \pm 0.012$, respectively. An average value $E_p = -0.468 \pm 0.010$ was adopted. This value represents the efficiency of the polarimeter for a 122 (or 129) keV line with no dilution from x rays. To be related to the ^{191}Ir efficiency it must be scaled by the factor $(1+g)^{-1}$. By comparing ^{57}Fe and ^{191}Ir polarimeter spectra (see Fig. 5), a value $g = 0.07 \pm 0.03$ was deduced, giving an efficiency $E_p = -0.437 \pm 0.015$. Combining this result with

the ^{191}Ir measurements yielded the adopted polarization efficiency $E_p = -0.435 \pm 0.015$.

F. Time-reversal asymmetry measurement

The experimental setup for the time-reversal runs is shown in Fig. 4. The asymmetry of Eq. (12) is measured by comparing polarimeter count rates for applied fields of opposite polarity ($\vec{B}$ and $-\vec{B}$). This technique has the advantage that rate differences are sought with no change in source or detector positions. The orienting field is reversed ($\theta \rightarrow \pi - \theta$, $\phi \rightarrow \pi + \phi$) by inverting the input to the voltage-controlled current supply driving the superconducting coils. The input switching waveform is controlled by a master timer. At time $t = 0$ data accumulation is stopped and field switching is initiated simultaneously with a dead time clock. The latter is set for a time interval generally chosen to be 1 or 2 min, in order to permit the source to cool back to its steady state value after the temperature increase caused by field reversal. A ramp time of 25 s was used for the switching waveform to further minimize this heating effect. At the end of the dead time the count gates are opened for the next counting period. Counting intervals of 10 min were normally implemented, sufficiently short to eliminate the effects of electronic drift.

The resulting series of alternate-field-polarity data were analyzed by computing the asymmetry

$$A_i' = [W_i'(+) - W_i'(-)]/[W_i'(+) + W_i'(-)] \tag{23}$$

for each pair of $(+,-)$ field counting rates, for each of the four polarimeter counters. (The counters are oriented so that $\phi_i = 45°$, 135°, 225°, and 315° for $i = 1$ to 4.) The W_i' again refer to the total integrated count rate in the window of Fig. 5, corrected for source decay. In actuality every run was compared to the average of the preceding and following runs in order to eliminate the influence of first order temperature and count rate drifts. The series A_i' were combined and averaged over counters, adjusting for the signs of counters 2 and 4 which view opposite polarization patterns relative to counters 1 and 3. Additionally, the asymmetry

$$A' = \frac{1}{8}\left[\frac{W_1'(+)W_2'(-)W_3'(+)W_4'(-)}{W_1'(-)W_2'(+)W_3'(-)W_4'(+)} - 1\right] \tag{24}$$

was computed for each pair of $(+,-)$ runs. As count rates proved to be quite stable, the two procedures for computing A' yielded nearly identical results. Under normal operation the normalized χ^2 was approximately equal to 1 for all runs.

The background contributes no asymmetry to the time-reversal asymmetry A', but dilutes the measured effect. The corrected asymmetry A of Eq. (12) is obtained from

$$A = A'(1 + f) \ , \tag{25}$$

where f is the ratio of background to signal in the integrated spectrum.

Time-reversal data were acquired for all four (N, S, E, and W) azimuthal polarimeter configurations, typically in pairs of 24 h runs at opposite positions (N and S, and E and W). This is equivalent to measuring the T-odd distribution $W_3(\theta,\phi)$ at (θ_m,ϕ_m) and $(\pi - \theta_m, \pi + \phi_m)$, and proved useful in detecting and averaging out small geometric or nonsymmetric-field-reversing effects.

IV. RESULTS

Four independent measurements with ^{191}Ir were performed. Experiment no. 1 was a preliminary measurement incorporating an older, less efficient version of the polarimeter ($E_p = -0.21$). The source for this experiment was a 0.013 mm thick Fe(Os) foil indium soldered to the copper collar button of the refrigerator's cooling rod. Data were acquired successively for E, W, N, and S polarimeter configurations.

Improvements in polarimeter shielding resulted in a factor of two gain in polarization efficiency for the subsequent experiments. The source used for experiment no. 2 was a 0.018 mm thick Fe(Os) foil, again indium soldered to copper. Data were acquired consecutively in NS and EW pairs of 24 h runs, and for different cyclic permutations of the four NaI counters located at $\phi = 45°$, 135°, 225°, and 315°, in order to average out small geometric effects. Raw asymmetries A' for the 29 consecutive runs are plotted in Fig. 6.

For this second source an anomalous orientation of the Ir nuclei, perpendicular to the foil plane, was observed when no external magnetic field was applied.[23] This orientation is attributed to magnetostrictive effects caused by the differential contraction of iron and copper at low temperatures. The iron experiences a net radial compression upon cooling, resulting in the magnetostrictively induced alignment of domains orthogonal to the foil plane. This

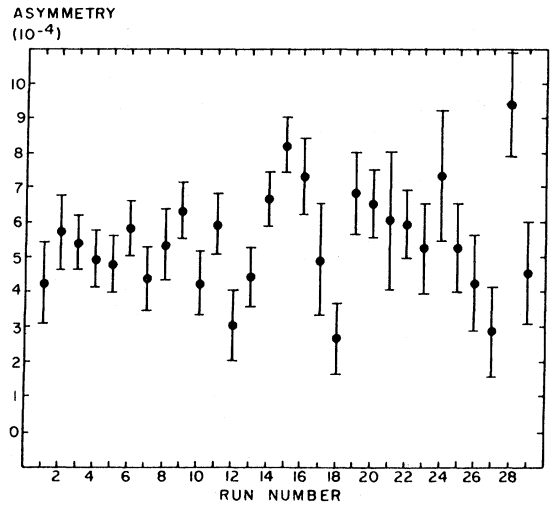

FIG. 6. Asymmetries of experiment no. 2. Each of the 29 individual runs is approximmately 12 h duration.

effect appears to be completely erased whenever the foil is saturated by an external field. However, to explore any unforseen influence of magnetostriction on our measurements, experiment no. 3 incorporated a new source collar button consisting of a 0.25 cm diameter platinum rod surrounded by a 0.25 mm thick copper sleeve. (The copper sleeve was found to be necessary to maintain sufficiently high thermal conduction at mK temperatures.) Platinum has a thermal expansion coefficient closer to iron than that of copper, and actually smaller than iron's. The Fe(Os) foil, indium soldered to the platinum collar button, therefore experiences a net radial expansion upon cooling. Under the condition of zero external field, this source exhibited the opposite magnetostrictive behavior of a net radial (in the foil plane) alignment of domains. However, no significant variation in source orientation parameters or time-reversal asymmetry measurements were observed, demonstrating the negligibility of magnetostrictive effects on the experiment. Experiment no. 4 reverted to a 0.0245 mm thick Fe(Os) foil soldered to copper.

The parameters of source temperature and polarization, polarization efficiencies and background-to-signal coefficients, the observed asymmetries, and the resulting phase angles for all four experiments are summarized in Table I. This table is a revised version of Table I of Ref. 11, which summarized the first three experiements, and incorporates the more recent polarization efficiency and background parameter determinations. Reflected in Table I are the increased source strengths of the final two experiments which resulted in higher source temperatures and lower polarization coefficients. Due to ^{192}Ir contaminants these sources also displayed significantly higher levels of background in the polarimeter spectra, as indicated by the larger f values.

Also summarized in Table I are the results of control experiments performed for sources 1 and 2 at 4 K. No systematic asymmetry was observed, demonstrating the absence of significant instrumental effects not dependent upon polarization.

The last column in Table I gives the phase shifts $(\eta + \xi)$, determined from the corrected asymmetry A via Eqs. (11) and (12):

TABLE I. Experimental results.

Experiment no.	Temperature T(K)	Polarization $f_a\langle B_3\rangle$	$f_a\langle B_4\rangle$	Polarization efficiency E_p	Background to signal f	Raw asymmetry A' (10^{-4})	Corrected asymmetry A (10^{-4})	Phase $\eta + \xi$ (10^{-3})
1	0.024	1.35(3)	1.0	−0.21(2)	0.03(2)	2.52(11)	2.60(13)	−4.46(48)
Control	4.0	0.0	0.0			0.09(17)		
2	0.025	1.31(3)	1.0	−0.435(15)	0.08(3)	5.40(19)	5.83(21)	−4.97(30)
Control	4.0	0.0	0.0			0.07(33)		
3	0.030	1.21(3)	0.9	−0.435(15)	0.45(8)	3.69(15)	5.36(37)	−4.94(40)
4	0.030	1.07(4)	0.7	−0.435(15)	0.21(5)	3.56(13)	4.29(24)	−4.48(34)
Weighted average								−4.76(21)

$$\sin(\eta+\xi) = A\,\frac{1+SQ_4f_aB_4P_4(\cos\theta_m)\,|\delta|^2/(1+|\delta|^2)}{RQ_3f_aB_3P_3(\cos\theta_m)E_p[\,|\delta|e^{i\pi}/(1+|\delta|^2)]} \tag{26}$$

$$= A\frac{1-(0.0128\pm0.0002)f_aB_4}{(0.203\pm0.001)f_aB_3E_p}\,. \tag{27}$$

To obtain Eq. (27) we have substituted $|\delta|e^{i\pi} = -0.399 \pm 0.004$, $Q_3 = 0.963$, $Q_4 = 0.940$, and numerical values for the spin coefficients $R = -0.1061$ and $S = 0.2556$.

Consistent values of $\sin(\eta+\xi) \simeq (\eta+\xi)$ are obtained for all experiments. From the weighted average of the four values a final result $(\eta+\xi) = (-4.76\pm0.21)\times10^{-3}$ is obtained. For subsequent discussions a value $(\eta+\xi) = (-4.8\pm0.2)\times10^{-3}$ is adopted.

V. DISCUSSION

The present observation of a nonvanishing value of $(\eta+\xi) = (-4.8\pm0.2)\times10^{-3}$ for the mixed 129 keV γ transition in ^{191}Ir may be explained in terms of atomic final state effects. In Ref. 11 we compared the experimental result with the available calculated final state phases of Goldwire and Hannon.[10] From their work we found a conversion phase shift $\xi_C = \xi_C(E2) - \xi_C(M1) = -4.51\times10^{-3}$ and a Thomson-scattering phase shift $\xi_R = \xi_R(E2) - \xi_R(M1) = 0.80\times10^{-3}$ between the two multipole components of the 129 keV transition. The total phase shift for the two final state processes was $\xi = \xi_C + \xi_R = -3.7\times10^{-3}$, with a quoted error of a few percent. Although of the same sign and order of magnitude, the calculated phase ξ differed from the measured $(\eta+\xi)$ by some five standard deviations. If it was assumed that no time-reversal violation of this magnitude was present, the experimental observation could not be reconciled with the calculated atomic final state phase shift. [Contributions from other known T-violation-simulating processes of "Faraday rotation" (see discussion in Ref. 6) and nuclear final state effects[8] are estimated to be $< 10^{-6}$ and negligible at the present level of precision.]

The discrepancy between calculation and measurement, apparent evidence for a time-reversal violation, has motivated the recent theoretical study of atomic final state effects by Davis *et al.*[9] Their calculations for ^{191}Ir yield conversion phase shifts ξ_C for the atomic K, L, M, and N shell electrons of -3.85×10^{-3}, -0.97×10^{-3}, -0.23×10^{-3}, and -0.05×10^{-3}, respectively, giving a total of $\xi_C = -5.10\times10^{-3}$. The phase shift for Rayleigh scattering (including Thomson scattering and the small anomalous scattering term) is $\xi_R = 0.79\times10^{-3}$. The total atomic final state phase shift then becomes $\xi = \xi_C + \xi_R = (-4.3\pm0.4)\times10^{-3}$ (the indicated error bars represent a 2% uncertainty for the $E2$ and $M1$ phases). Our measured value is in agreement with the given upper limit of -4.7×10^{-3}. The revised calculations thus remove the apparent evidence for violation of time-reversal invariance.

Experimental confirmation of atomic final state effects in nuclear transitions is obtained from Mossbauer experiments. Such experiments are sensitive to a dispersion term in the absorption cross section proportional to ξ_D, with

$$\xi_D = [\xi(M1) + |\delta|^2\xi(E2)]/(1+|\delta|^2)\,,$$

rather than the direct phase shift $\xi = \xi(E2) - \xi(M1)$. In Ref. 9, Davis *et al.* list the results of dispersion measurements for various transitions together with the calculated values for ξ_D. Agreement between experiment and theory is in general quite good. Included is the result of a Mossbauer experiment which also measured the 129 keV transition in ^{191}Ir; a value $\xi_D = (-0.50\pm0.12)\times10^{-3}$ is to be compared to the calculated $\xi_D = -0.69\times10^{-3}$. The measurement ξ_D is sensitive to a combination of $M1$ and $E2$ phases nearly orthogonal to the T-violation-simulating phase ξ, however, and no comparison can be made with the present observation. We note that similar time-reversal experiments yielding $(\eta+\xi) = (-0.3\pm0.6)\times10^{-3}$ and $(-1.2\pm1.1)\times10^{-3}$ for the 122 and 364 keV transitions in ^{57}Fe (Ref. 5) and ^{131}Xe,[24] respectively, are essentially null results, consistent with the small calculated phases of -0.6×10^{-3} and -0.1×10^{-3} for those two transitions. Further investigation of final state effects in other suitable nuclear transitions would be desirable.

In conclusion, by measuring the linear polarization of the mixed 129 keV γ ray in ^{191}Ir oriented in iron, we have established for the first time a nonvanishing T-odd angular correlation in a nuclear transition. The ratio of transition amplitudes for the two competing multipoles was found to have an imaginary component with a corresponding phase angle of $(-4.8\pm0.2)\times10^{-3}$. This time-reversal-like phase shift may be attributed to virtual quantum

electrodynamic effects in the atomic final state, and is now accounted for by the final state calculations of Ref. 9. The precision of the measurement is half an order of magnitude greater than all previous time-reversal measurements in low energy nuclear physics. Assuming the validity of the theoretical bounds $-3.9 \times 10^{-3} \leq \xi \leq -4.7 \times 10^{-3}$ of Ref. 9, a limit $|\eta| \leq 10^{-3}$ may be inferred, consistent with time-reversal invariance.

ACKNOWLEDGMENTS

We wish to acknowledge the help of S. Kellogg, N.H. Kwong, and E. Redden with the experiment. Thanks are due to P. Herczeg, P. Vogel, and B. R. Davis for many helpful discussions. This work was supported by the U. S. Department of Energy under Contract No. DEAT0381-ER40002.

---

*Present address: Bell Laboratories, Holmdel, N.J. 07733.

[1]J. H. Christenson, J. W. Cronin, V. L. Fitch, and R. Turlay, Phys. Rev. Lett. 13, 138 (1964).

[2]R. C. Casella, Phys. Rev. Lett. 21, 1128 (1968); 22, 554 (1969).

[3]K. Kleinknecht, Annu. Rev. Nucl. Sci. 26, 1 (1976).

[4]S. P. Lloyd, Phys. Rev. 81, 161 (1951).

[5]N. K. Cheung, H. E. Henrikson, E. J. Cohen, A. J. Becker, and F. Boehm, Phys. Rev. Lett. 37, 588 (1976).

[6]N. K. Cheung, H. E. Henrikson, and F. Boehm. Phys. Rev. C 16, 2381 (1977).

[7]J. P. Hannon and G. T. Trammell, Phys. Rev. Lett. 21, 726 (1968).

[8]E. M. Henley and B. A. Jacobsohn, Phys. Rev. Lett. 16, 706 (1966).

[9]B.R. Davis, S. E. Koonin, and P. Vogel, Phys. Rev. C 22, 1233 (1980).

[10]H. C. Goldwire, Jr. and J. P. Hannon, Phys. Rev. B 16, 1875 (1977).

[11]J. L. Gimlett, H. E. Henrikson, N. K. Cheung, and F. Boehm, Phys. Rev. Lett. 42, 354 (1979).

[12]R. M. Steffen, Los Alamos Scientific Laboratory Report No. LA-4565-MS, 1971 (unpublished).

[13]R. M. Steffen and K. Alder, in *The Electromagnetic Interaction in Nuclear Spectroscopy,* edited by W. D. Hamilton (North-Holland, Amsterdam, 1975), p. 505.

[14]K. S. Krane, Los Alamos Scientific Labortory Report No. LA-4677, 1971 (unpublished).

[15]K. S. Krane, Nucl. Data Tables 11, 407 (1973).

[16]D. Salomon and D. A. Shirley, Phys. Rev. B 9, 29 (1974).

[17]G. Eska, E. Hagn, T. Butz, and P. Kienle, Phys. Lett. 36B, 328 (1971), report a value $\mu = 6.03\mu_N$ for an NMR measurement sensitive to the product of μ and $B_{\rm hf}$, taking $B_{\rm hf} = 1.405$ MG. Assuming the more recent value $B_{\rm hf} = 1.481$ MG of Ref. 16, μ becomes $\mu = 5.72$.

[18]K. S. Krane, At. Data Nucl. Data Tables 18, 137 (1976); K. S. Krane and W. A. Steyert, Phys. Rev. C 7, 1555 (1973).

[19]A. J. Becker, H. E. Henrikson, and D. C. Cook, Nucl. Instrum. 108, 291 (1973).

[20]K. S. Krane and W. A. Steyert, Phys. Rev. C 9, 2063 (1974).

[21]E. Matthias and R. J. Holliday, Phys. Rev. Lett. 17, 897 (1966).

[22]E. J. Cohen, A. J. Becker, N. K. Cheung, and H. E. Henrikson, Hyperfine Int. 1, 193 (1975).

[23]J. L. Gimlett, Ph. D. thesis, 1980, California Institute of Technology (unpublished).

[24]J. L. Gimlett, H. E. Henrikson, G. Lerner, and F. Boehm, Phys. Rev. C (to be published).